Imaging the Effects of Prostaglandin Analogues on Cultured Trabecular Meshwork Cells by Coherent Anti-Stokes Raman Scattering

Tim C. Lei,[1] Omid Masihzadeh,[2] Malik Y. Kahook,[2] and David A. Ammar[2]

[1]Department of Electrical Engineering, University of Colorado Denver, Denver, Colorado
[2]Department of Ophthalmology, University of Colorado Denver, Aurora, Colorado

Correspondence: David A. Ammar, University of Colorado Medical School, Department of Ophthalmology, Mail Stop #8311, 12800 East 19th Avenue, Room #5105, Aurora, CO 80045; David.Ammar@ucdenver.edu.

Submitted: March 19, 2013
Accepted: July 23, 2013

Citation: Lei TC, Masihzadeh O, Kahook MY, Ammar DA. Imaging the effects of prostaglandin analogues on cultured trabecular meshwork cells by coherent anti-Stokes Raman scattering. *Invest Ophthalmol Vis Sci*. 2013;54:5972–5980. DOI:10.1167/iovs.13-12065

Purpose. The aim of this study was to nondestructively monitor morphological changes to the lipid membranes of primary cultures of living human trabecular meshwork cells (hTMC) without the application of exogenous label.

Methods. Live hTMC were imaged using two nonlinear optical techniques: coherent anti-Stokes Raman scattering (CARS) and two-photon autofluorescence (TPAF). The hTMC were treated with a commercial formulation of latanoprost (0.5 μg/mL) for 24 hours before imaging. Untreated cells and cells treated with vehicle containing the preservative benzalkonium chloride (BAK; 2 μg/mL) were imaged as controls. After CARS/TPAF imaging, hTMC were fixed, stained with the fluorescent lipid dye Nile Red, and imaged by conventional confocal microscopy to verify lipid membrane structures.

Results. Analysis of CARS/TPAF images of hTMC treated with latanoprost revealed multiple intracellular lipid membranes absent from untreated or BAK-treated hTMC. Treatment of hTMC with sodium fluoride or ouabain, agents shown to cause morphological changes to hTMC, also did not induce formation of intracellular lipid membranes.

Conclusions. CARS microscopy detected changes in living hTMC morphology that were validated by subsequent histological stain. Prostaglandin-induced changes to hTMC involved rearrangement of lipid membranes within these cells. These in vitro results identify a novel biological response to a class of antiglaucoma drugs, and further experiments are needed to establish how this effect is involved in the hypotensive action of prostaglandin analogues in vivo.

Keywords: trabecular meshwork cells, prostaglandin analogs, coherent anti-Stokes Raman scattering (CARS)

Prostaglandin analogues (PGAs) are both the first-line and most commonly prescribed treatment for primary open-angle glaucoma.[1] PGAs decrease intraocular pressure even under conditions in which the iridocorneal angle is closed or otherwise occluded.[2,3] Histological data show an increase in the size and number of spaces within the ciliary muscle with PGA treatment.[4] From these and other findings, it has been presumed that PGAs act primarily by enhancing the uveoscleral outflow of aqueous humor (AH). Recent evidence suggests that PGAs can also act directly on the human trabecular meshwork (TM) and Schlemm's canal to facilitate AH exit through the conventional outflow pathway.[5,6] However, compared to our understanding of the effect of PGAs on uveoscleral outflow, PGA regulation of conventional outflow is less well understood.

In order to better understand the effects of PGAs on the conventional outflow pathway, we examined the biological response of primary cultures of human trabecular meshwork cells (hTMC) to the PGA latanoprost. We used two multiphoton microscopy (MPM) techniques: two-photon autofluorescence (TPAF) and coherent anti-Stokes Raman scattering (CARS). TPAF has become a ubiquitous laboratory tool for nondestructive imaging of live cells in culture.[7,8] In TPAF, pulsed laser light generates a fluorescent signal through simultaneous absorption of two photons, unlike traditional fluorescent confocal microscopy that generates a fluorescent signal through absorption of a single photon. Compared to single-photon microscopy, TPAF offers reduced photodamage due to the longer wavelength of the excitation laser while still offering intrinsic axial cross sectioning.[8,9] We have previously used TPAF to detect NAD(P)H in live cultures of primary human TM cells (hTMC).[10] In this study we have also employed CARS microscopy, another MPM technique based on the vibrational properties of molecules.[11–14] In practice, CARS detects carbon-hydrogen bonds of lipid molecules as a label-free image contrast for imaging cellular membranes. CARS, therefore, has the unique ability to image the hydrocarbon/lipid-rich membranes as well as lipid-based biological processes in living cells.[15–18] Using simultaneous CARS/TPAF microscopy, we have detected latanoprost-induced changes to hTMC that to our knowledge have not been previously described. These findings suggest a new avenue for investigating the hypotensive action of PGAs in vivo.

Materials and Methods

Reagents

Primary hTMC, isolated from the juxtacanalicular and corneoscleral regions of the human eye, and culture media (Fibroblast Medium; FM) were purchased from ScienCell Research Laboratories (Carlsbad, CA). FM consisted of a proprietary basal medium formulation supplemented with 2% fetal bovine serum (FBS), a solution containing a proprietary mix of growth factors (fibroblast growth supplement), and penicillin/streptomycin. Rat tail type I collagen was purchased from Becton Dickson Biosciences (San Jose, CA). Phosphate-buffered saline (PBS; 8 g/L sodium chloride, 0.2 g/L potassium phosphate monobasic, 2.16 g/L sodium phosphate dibasic heptahydrate, pH 7.4), Alexa Fluor 488–labeled phalloidin, and Nile Red were purchased from Life Technologies (Carlsbad, CA). Sodium fluoride and ouabain were purchased from Sigma-Aldrich (St. Louis, MO). Fluorescein isothiocyanate–labeled anti-human β1-integrin (eBioscience, Inc., San Diego, CA) was a gift of Karen B. King (University of Colorado Denver, Denver, CO). Benzalkonium chloride was purchased from Acros/Thermo Fisher Scientific (Waltham, MA). An ophthalmic solution containing 50 μg/mL latanoprost along with 200 μg/mL benzalkonium chloride (BAK; 0.02% w/v) as a preservative was purchased from Pfizer (Xalatan; New York, NY).

Prostaglandin and Control Drug Treatment

Prior to use, 35-mm glass-bottom culture dishes (MatTek Corporation, Ashland, MA) and 18-mm glass coverslips were coated with 50 μg/mL collagen. The hTMC were then plated at a density of 2000 cells/cm^2 and allowed to adhere for 2 to 3 hours. For PGA treatment, media were exchanged for fresh FM containing a 1:100 dilution of a commercial formulation of latanoprost (final concentration, 0.5 μg/mL latanoprost and 2 μg/mL BAK). Untreated hTMC were exchanged to fresh FM, and BAK-treated hTMC were exchanged to fresh FM containing 2 μg/mL BAK. All hTMC were cultured for an additional 24 hours before imaging or staining. In some experiments, untreated hTMC were exposed to either 300 nM ouabain for the final 2 hours or 40 mM sodium fluoride (NaF) in the last 30 minutes before live imaging.

Imaging of Filamentous Actin in hTMC

The hTMC grown on collagen-coated glass coverslips were treated with latanoprost or control solutions for 24 hours. After rinsing in PBS, hTMC were fixed for 1 hour in 4% paraformaldehyde in PBS (w/v), washed three times in PBS, incubated in PBS containing 0.01% Triton X-100, and then blocked in PBS containing 2% BSA overnight. The hTMC were then incubated in 0.2 μM Alexa Fluor 488 phalloidin in PBS for 30 minutes, washed three times in PBS, and mounted on slides in Vectashield Mounting Media (Vector Laboratories, Burlingame, CA). Slides were placed on a Nikon Eclipse 80i microscope (Nikon, Melville, NY) equipped with the NIS Elements control software (Nikon). Alexa 488 phalloidin–labeled filamentous actin was imaged using an excitation filter (465–500 nm band pass) and emission filter (516–556 nm band pass; Semrock, Inc., Rochester, NY). Images (pixel resolution 960 × 1280) were collected with a Nikon 20×/0.50 numerical aperture (NA) Plan Fluor objective lens using a Nikon DS-Qi1 monochrome camera.

Imaging Live hTMC by CARS/TPAF Multiphoton Microscopy

Coherent anti-Stokes Raman scattering and TPAF images were acquired with a custom-built MPM platform optimized for CARS and TPAF imaging (Advanced Light Microscopy Core Facility, University of Colorado-Denver, Denver, CO). A detailed description is supplied in our previous work.[19] In brief, the laser system (picoEMERALD; HighQ Laser, Rankweil, Austria) consisted of a 10-watt diode-pumped Nd:Vanadate ($Nd:YVO_4$) picosecond (ps) laser at a repetition rate of 80 MHz. Inside the system, 9 watts of the generated 1064-nm laser beam was redirected to a frequency-doubling crystal to produce 5 watts of 532-nm light, which was subsequently sent into an optical parametric oscillator to convert the 532-nm laser beam into a 1-watt, ~6 ps, 816-nm laser beam. The remaining 1 watt of the 1064-nm beam (Stokes) from the $Nd:YVO_4$ laser was then optically recombined with the 816-nm optical beam (Pump and Probe) and sent into an inverted Olympus FV-1000 confocal microscope platform (Olympus, Center Valley, PA) for CARS and TPAF imaging (Fig. 1). The powers of the two laser beams delivered to the microscope were adjusted inside the laser system. For these experiments, the optical power at the objective (UPSLAPO 60× IR W; Olympus) was 12.4 mW for the 816-nm laser beam and 11.25 mW for the 1064-nm laser beam; both settings are below the tissue damage threshold.[20]

The hTMC grown on collagen-coated 35-mm glass-bottom dishes were rinsed with PBS and placed on the microscope stage in a humidity/temperature-controlled chamber (INUB-G2A-ZILCS; Tokai Hit, Fujinomiya, Japan). Live hTMC were imaged using a 60× 1.2 NA water objective (UPLSAPO 60× IR W; Olympus) optimized for CARS and TPAF imaging. TPAF signal (between 420 and 520 nm) was collected in the reverse (epi) direction through the objective lens using an emission filter (hp470/100m-2p; Chroma Technology, Bellows Falls, VT) in front of a photomultiplier detector. CARS signal was collected with a second emission filter (hq660/40m-2p) located in front of a forward photomultiplier detector. The Olympus FV-1000 software package was used to collect all MPM images. The pixel dwell time was 10 μs and the image pixel resolution was 1024 × 1024. A Kalman line average filter (n = 3) was applied during image acquisitions to improve the signal-to-noise ratio of the acquired images.

Nile Red Staining

A stock solution of Nile Red was prepared at 0.5 mg/mL in acetone. After CARS imaging, hTMC treated with latanoprost and control solutions were fixed for 1 hour in 4% paraformaldehyde in PBS (w/v), washed three times in PBS, and then incubated overnight in PBS containing 50 mM NH_4Cl in order to quench autofluorescence from free aldehyde groups. The hTMC were then incubated for 30 minutes in PBS containing 5 μg/mL Nile Red (1:100 dilution of stock solution), washed in PBS three times for 30 min, and rinsed with distilled water. The glass coverslips were removed from the 35-mm culture dish with a razor blade and mounted in distilled water onto glass slides and immediately imaged (see below).

Integrin Staining

The hTMC grown on collagen-coated glass coverslips were treated with latanoprost for 24 hours. After rinsing in PBS, hTMC were fixed for 1 hour in 4% paraformaldehyde in PBS (w/v), washed three times in PBS, incubated in PBS containing 0.01% Triton X-100 for 30 minutes, and then incubated in PBS containing 2% BSA overnight. The hTMC were incubated in 2.5 μg/mL fluorescein-conjugated anti-β1 integrin in PBS/2% BSA for 1 hour, washed three times in

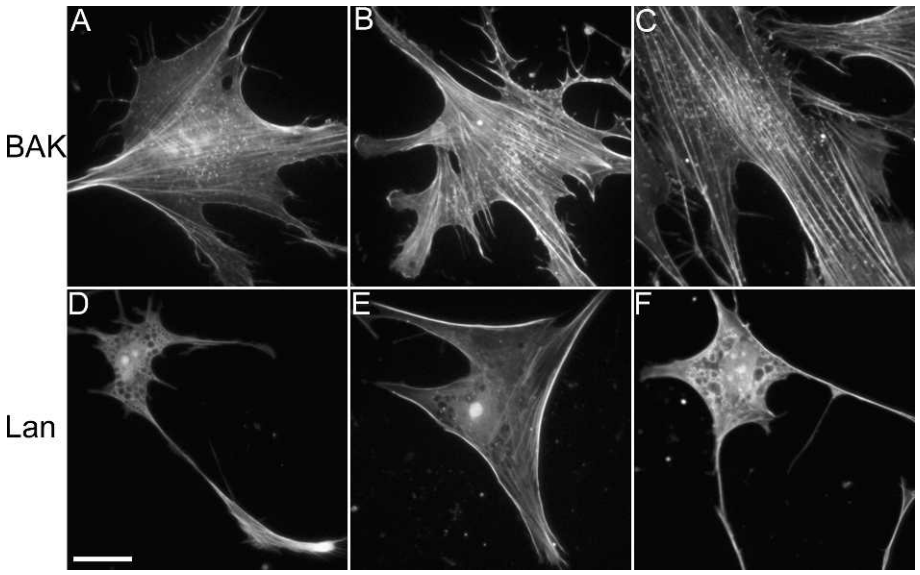

FIGURE 1. Latanoprost treatment reduces filamentous actin in primary cultures of human trabecular meshwork cells (hTMC). Live cells were treated with 2 μg/mL benzalkonium chloride (BAK [**A–C**]) or 0.5 μg/mL latanoprost and 2 μg/mL BAK (Lan [**D–F**]) for 24 hours, then fixed and stained with fluorescent phalloidin to label the filamentous actin structures. *Scale bar*: 20 μm.

PBS, and then mounted on slides in Vectashield Mounting Media (Vector Laboratories).

Laser Confocal Microscopy of Nile Red– and Anti-Integrin–Stained hTMC

The hTMC mounted on glass slides were placed on an adapted confocal microscope (LSM 510 META on Axiovert 200M platform) and imaged using a Plan-Apochromat 63×/1.4 NA oil objective (Carl Zeiss MicroImaging, Inc., Göttingen, Germany). The 543-nm line of the helium/neon laser (10% power) was used as an excitation source along with a band-pass emission filter (565–615 nm) to visualize Nile Red fluorescence. The 488-nm line of the argon/krypton laser (2% power) was used as an excitation source along with a band-pass emission filter (500–530 nm) to visualize the fluorescein-conjugated anti-β1 integrin antibody. Images were collected using a line-scan average ($n = 4$) via the Zeiss ZEN 2009 control software (Carl Zeiss MicroImaging, Inc.). The pixel dwell time was 0.8 μs and the image pixel resolution was 2048 × 2048.

Image Analysis and Processing

Acquired images were postprocessed for background noise (nonresonant background) reduction and prepared in its current format by ImageJ (http://rsbweb.nih.gov/ij/; provided in the public domain by National Institutes of Health, Bethesda, MD) software, which was also used to perform surface-area measurements (using the freehand tool) and focal adhesion counting (using the image-based tool for counting nuclei).

RESULTS

Latanoprost Treatment Induces Cytoskeletal Changes to Primary hTMC

The hTMC used in all experiments were isolated from the juxtacanalicular and corneoscleral regions of human eyes. It has been independently verified that dexamethasone induces myocilin expression in these cells,[21] a characteristic response of TM cells to glucocorticoids.[22] The ophthalmic preparation of PGA used in these experiments contains both latanoprost and a detergent preservative (BAK). In order to examine the effects of both components of this ophthalmic preparation on actin stress fibers, hTMC were fixed and stained with fluorescent phalloidin, which preferentially binds to polymerized actin. Stress fibers containing long continuous strands of filamentous actin were apparent in both BAK (2 μg/mL)-treated cells (Fig. 1) and untreated controls (data not shown). In cells treated with both 0.5 μg/mL latanoprost and 2 μg/mL BAK (Lan), filamentous actin staining was greatly diminished. In addition, hTMC appeared much smaller after latanoprost treatment. Also visible were small round structures within latanoprost-treated hTMC that lacked fluorescence. The cytoplasm of cells usually contains short oligomeric actin, yielding a faint fluorescent background when stained with fluorescent phalloidin. The lack of fluorescence within these spherical structures suggests that they are separated from the cytoplasm by lipid membrane.

Latanoprost Treatment Induces Intracellular Structures Within hTMC That Are Rich in Lipids

Live hTMC were imaged by CARS/TPAF microscopy to determine the structural changes that occur with latanoprost treatment. Figure 2 shows untreated hTMC (CNT) and hTMC treated with 2 μg/mL BAK (BAK). CNT and BAK-treated hTMC have a similar flattened appearance. The CARS microscopic images show the outline of the hTMC "footprint," and these are qualitatively similar in BAK and CNT cells (Fig. 2, arrowhead). The circular or oval structure within the center of these cells is very likely to be the cell nucleus (Fig. 2, asterisk). Small (<1 μm) lipid-rich structures (CARS signal in red) are visible in both CNT and BAK-treated hTMC, and these most likely represent intracellular microsomal vesicles (Fig. 2, arrows). We also detected signal by TPAF (green) from these cultures of hTMC, which we determined in our previous work to result from mitochondrial NAD(P)H fluorescence.[10] NAD(P)H is predominantly localized to the mitochondria, but does exist in other cellular locations. As a result, the TPAF fluorescent excitation of NAD(P)H in both CNT and BAK-

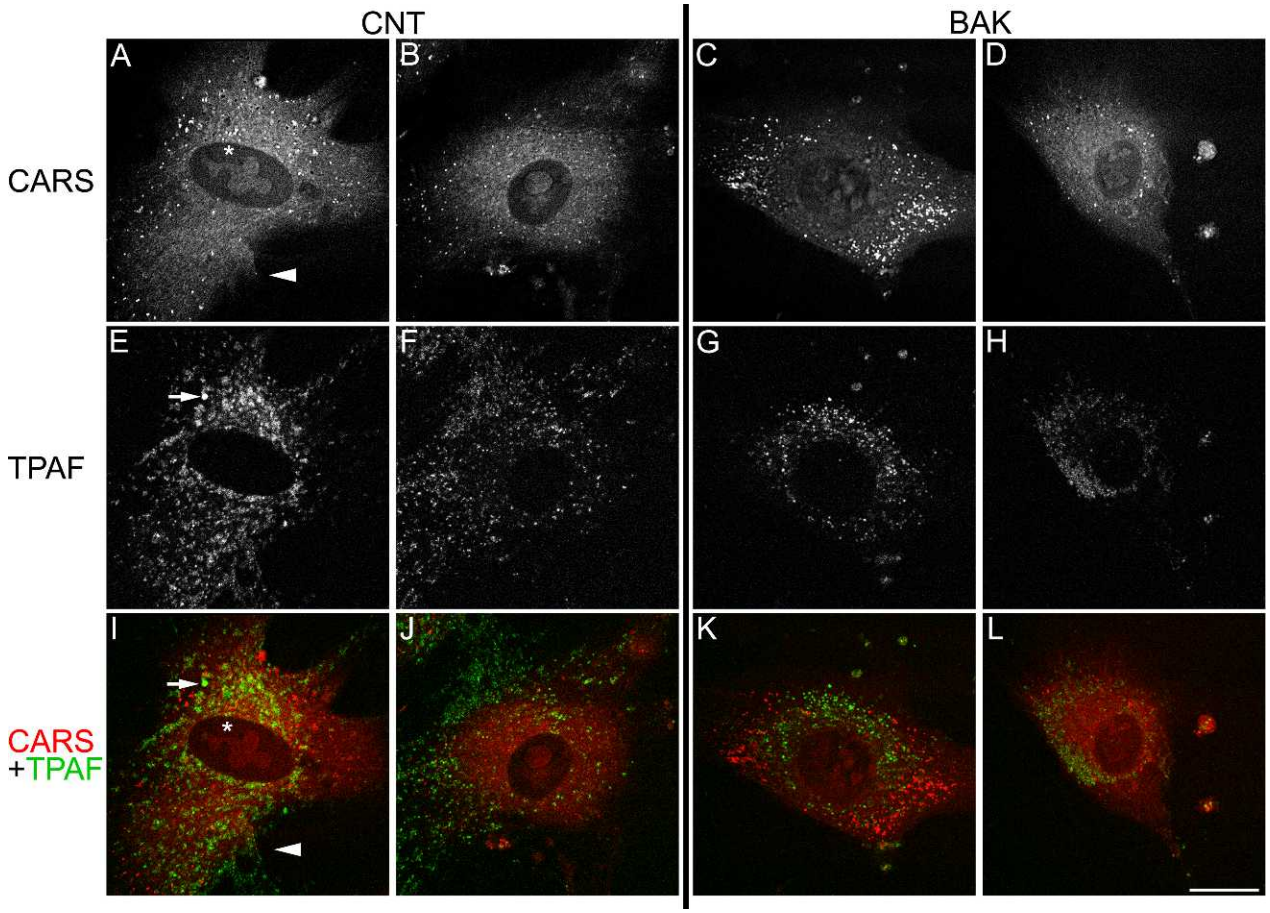

FIGURE 2. Human trabecular meshwork cells (hTMC) visualized by coherent anti-Stokes Raman scattering (CARS) and two-photon autofluorescence (TPAF). The CARS signal in live untreated cells (CNT [**A**, **B**]) or cells treated with 2 μg/mL benzalkonium chloride (BAK [**C**, **D**]) show an extended lipid footprint (*arrowheads*). The circular or oval structures within the center of these cells (visible in the *red* CARS channel) are likely the cell nuclei (*asterisk*). The small punctate structures detected by the *green* TPAF channel (*arrows*) derive from mitochondrial NAD(P)H fluorescence (**E**–**H**). Combined CARS/TPAF signals are shown in (**I**–**L**). *Scale bar*: 20 μm.

treated hTMC shows a bright punctate mitochondrial signal as well as a fainter cytosolic signal (Fig. 2). The punctate mitochondria signal is distributed fairly evenly throughout the hTMC, with a slightly higher number of mitochondria situated around the nucleus in the presumed neighborhood of the endoplasmic reticulum and Golgi (Fig. 2, arrow).

Live hTMC treated with 0.5 μg/mL latanoprost/2 μg/mL BAK (Lan) are shown in Figure 3 and exhibit remarkable changes in comparison to untreated (CNT) or BAK-treated hTMC (Fig. 2). The latanoprost-treated hTMC appear much more rounded and smaller in size, and the extended cell "footprint" that was seen with BAK and CNT cells is absent in cells treated with latanoprost. This footprint was reduced by 60% to 80% with latanoprost treatment, from ~1700 ± 500 μm^2 in CNT cells ($n = 12$) to ~550 ± 200 μm^2 in Lan cells ($n = 12$). Multiple spherical structures (between ~2 and 8 μm) are visible in the CARS channel (hollow ring-like structures) with latanoprost treatment (Figs. 3A–C, asterisk), suggesting that these structures are lipid in origin. The TPAF signal in the latanoprost-treated hTMC is still punctate (Figs. 3D–F) but can appear brighter due to being concentrated within a smaller cross-sectional area (because of cell rounding). We also note that in the panels combining CARS+TPAF signal, the green fluorescent signal from the mitochondria is not found within the spherical lipid structures (Figs. 3G–I, asterisk). This is better illustrated in Figure 4, which shows a higher-resolution latanoprost-treated hTMC. At this magnification, it is more apparent that the intracellular vesicles that appear with latanoprost treatment do not contain appreciable TPAF fluorescence.

We also examined the effect of 0.5 μg/mL latanoprost/2 μg/mL BAK (Lan) in live hTMC grown to a higher density. In separate experiments, hTMC were grown for 24 hours before the 24-hour exposure to PGA (for a total of 48 hours in culture). CARS images from the higher-density (30%–50%) hTMC cultures are shown in Figure 5. The lipid structures of control cells (CNT, Figs. 5A, 5C) appear quantitatively similar to the structures in the CNT cells shown in Figures 2A and 2B.

We subsequently used CARS microscopy to examine hTMC treated briefly with either ouabain or NaF to see if these agents could induce lipid-specific morphological changes similar to latanoprost treatment. Ouabain, a powerful inhibitor of the sodium-potassium transporter (Na/K-ATPase), has been shown to cause cell rounding and actin filament rearrangement in TM cells at 300 nM.[23] NaF (40 mM) causes the formation of actin stress fibers in fibroblast through activation of Rho,[24] a pathway critical to controlling TM cell shape and currently being investigated as a possible new target for glaucoma therapy.[25] We could not detect intracellular lipid structures in hTMC after exposure to either of these agents (Fig. 6), although ouabain did disrupt the F-actin (data not shown). These results suggest that the spherical structures seen in Figures 3 and 4 are

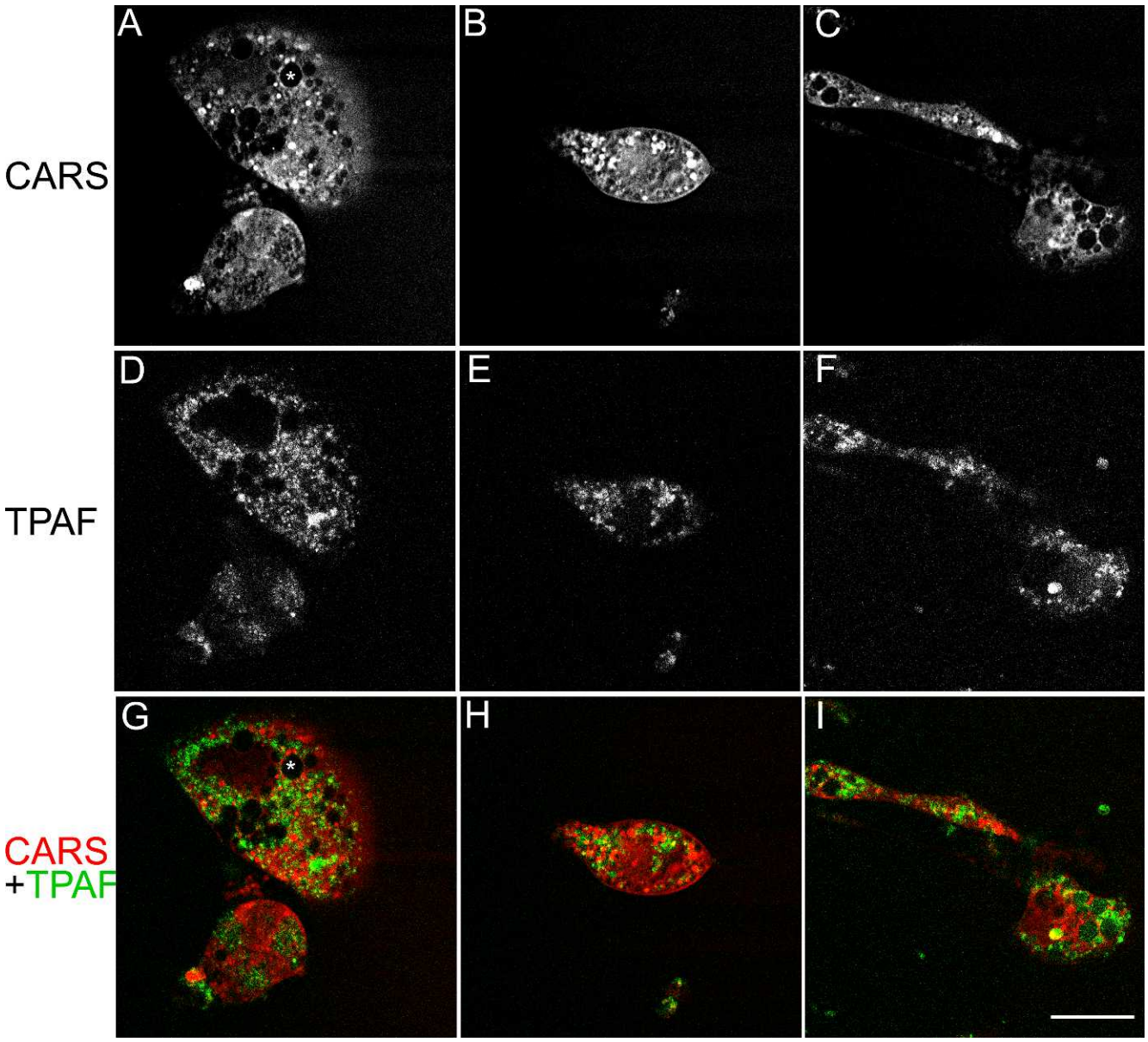

FIGURE 3. Latanoprost treatment causes the appearance of intracellular structures within human trabecular meshwork cells (hTMC). Live cells were visualized by coherent anti-Stokes Raman scattering (CARS) and two-photon autofluorescence (TPAF) after 24-hour treatment with 0.5 μg/mL latanoprost and 2 μg/mL BAK. Hollow ring-like structures (*asterisk*) between ~2 and 8 μm in diameter are visible in the CARS (*red*) channel with latanoprost treatment (**A–C**) that are not apparent in untreated cells (CNT, Figs. 2A, 2B) or cells treated with 2 μg/mL benzalkonium chloride alone (BAK, Figs. 2C, 2D). The punctate TPAF signal (*green*) from the mitochondrial NAD(P)H is visible (**D–F**). *Scale bar*: 20 μm.

not a direct result of actin filament assembly/disassembly and cell rounding, but may be specifically formed by latanoprost exposure. Additionally, the TPAF signal from the mitochondria of ouabain- and NaF-treated hTMC appears qualitatively the same as the TPAF signal from untreated cells (CNT) in Figure 1.

Intracellular Structures That Appear With Latanoprost Treatment Stain With Fluorescent Lipophilic Dye

In order to verify that the structures visible by CARS were lipid structures, hTMC were stained with a lipophilic fluorescent dye. After CARS imaging, cells were fixed and then incubated with a solution of Nile Red, a benzophenoxazinone that becomes intensely fluorescent in lipid-rich environments.[16,26] Using confocal laser scanning microscopy, latanoprost-treated hTMC (Lan) showed spherical fluorescent structures (Fig. 7) similar to those seen with CARS microscopy (Figs. 3, 4). In agreement with the CARS microscopy shown in Figure 2, no such intracellular structures could be seen in untreated (CNT) or BAK-treated hTMC stained with Nile Red (Fig. 7).

Changes in Focal Adhesions in hTMC With Latanoprost Treatment

The hTMC were treated with latanoprost for 24 hours and then fixed and stained with a fluorescent antibody for β1 integrin, a major cellular component for focal adhesions (FA). FA are sites where clusters of membrane proteins (integrins) bind to proteins within the extracellular matrix (such as fibronectin,

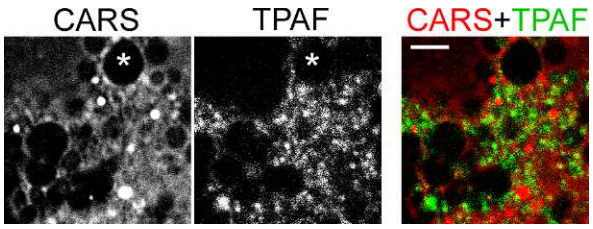

FIGURE 4. Higher magnification of the latanoprost-induced lipid structures within a human trabecular meshwork cell (hTMC). In a higher-resolution image of a latanoprost-treated hTMC, the CARS signal clearly shows the appearance of spherical intracellular structures (hollow ring-like structures, *asterisk*). The punctate TPAF signal from the mitochondrial NAD(P)H is also visible, but fluorescence is not present within these hollow ring-like structures (CARS+TPAF). *Scale bar*: 5 μm.

laminin, and collagen), serving as mechanical and structural linkages between cell and growth substrate. FA were detected using an antibody for β1-integrin, which previous studies have shown to be present in the FA of TM cells and involved in TM cell adhesion and cell spreading.[27–29] Using the number of FA as a metric for cell attachment, untreated hTMC cells contacted a region of the collagen-coated culture surface ~2050 μm^2 (Fig. 8, CNT). In agreement with the area measurement from CARS images, latanoprost-treated hTMC had an attachment area of only ~30% of the area of untreated controls (~575 μm^2, $n = 3$) (Fig. 8, Lan). While this reduced attachment area reduces the total number of FA per cell, the density of FA remaining in latanoprost-treated cells was increased slightly (16.0 ± 4.4 per 100 μm^2) compared to untreated hTMC (10.0 ± 1.6 per 100 μm^2, $n = 3$), indicating that latanoprost treatment does not specifically reduce hTMC attachment.

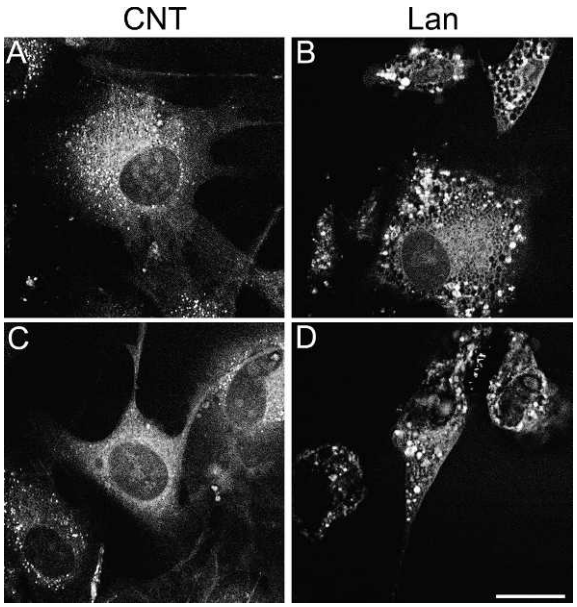

FIGURE 5. Latanoprost treatment in more confluent human trabecular meshwork cells (hTMC). hTMC were grown for 24 hours before 24-hour exposure to 0.5 μg/mL latanoprost (Lan). Cells were visualized by coherent anti-Stokes Raman scattering (CARS). CNT cells (**A**, **C**) appear quantitatively similar to lower-confluence CNT cells in Figures 2A and 2B. Additionally, Lan cells (**B**, **D**) demonstrated intracellular lipid vesicles seen with lower-confluence Lan cells in Figures 3A and 3C. *Scale bar*: 20 μm.

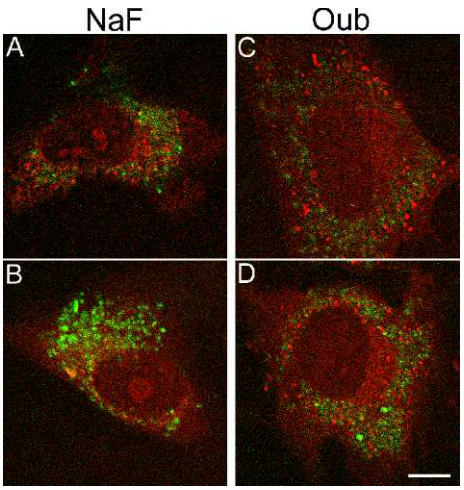

FIGURE 6. Sodium fluoride (NaF) or ouabain (Oub) treatments do not cause appearance of intracellular lipid structures. Human trabecular meshwork cells were treated with agents known to change morphology and actin cytoskeleton and then visualized by CARS (*red*). Cells treated with NaF (**A**, **B**) and Oub (**C**, **D**) appear similar to untreated cells (CNT, Figs. 2I, 2J). The TPAF signal (*green*) from the mitochondria is also visible. *Scale bar*: 20 μm.

DISCUSSION

MPM has the ability to image the function and structure of cells and tissues without exogenous dyes. This label-free imaging relies on simultaneous interactions of multiple photons with a target material. These interactions involve a resonant or nonresonant excitation of one of the basic energy states: electronic or vibrational energies. Unlike traditional microscopy in which a single photon interacts with material (through scattering or absorption), MPM uses pulsed infrared laser light to generate signal from a sample through simultaneous absorption or scattering of two or more photons. In TPAF, two photons from a single laser are simultaneously absorbed and excite the molecule to its higher electronic state. After nonradiative relaxation, the molecule returns to its electronic ground state through the release of a fluorescent photon. In CARS, two laser beams with different optical wavelengths simultaneously and resonantly excite the vibrational states of carbon-hydrogen bonds in an ensemble of lipid molecules in a coherent fashion. This ultimately results in the release of optical photons in a direction that is dependent on the size and shape of the lipid object. In most instances, however, significant CARS signal is emitted in the forward direction.[11,30]

The major site of aqueous outflow resistance is the juxtacanalicular region of the TM and inner wall of Schlemm's canal. Recent studies using Rho-kinase inhibitors have demonstrated that morphological changes to the endothelial cells of the TM can influence aqueous flow.[31] While the endothelial cells of the inner wall of Schlemm's canal exist as a continuous sheet, the TM cells within the juxtacanalicular region are clearly not confluent. Previous work documenting the effects of PGAs on TM cells has focused primarily on modeling confluent cultures. In contrast, our goal was to understand the effects of PGAs on hTMC at subconfluent conditions in order to model PGA effects on the juxtacanalicular or cribriform region of the TM. Therefore, we chose to examine single TM cells as well as cells at low confluence (30%–50% confluence) in our experiments.

In our previous work we have used the MPM techniques TPAF and second harmonic generation (SHG) to create high-resolution images of the tissue structures of the cornea,

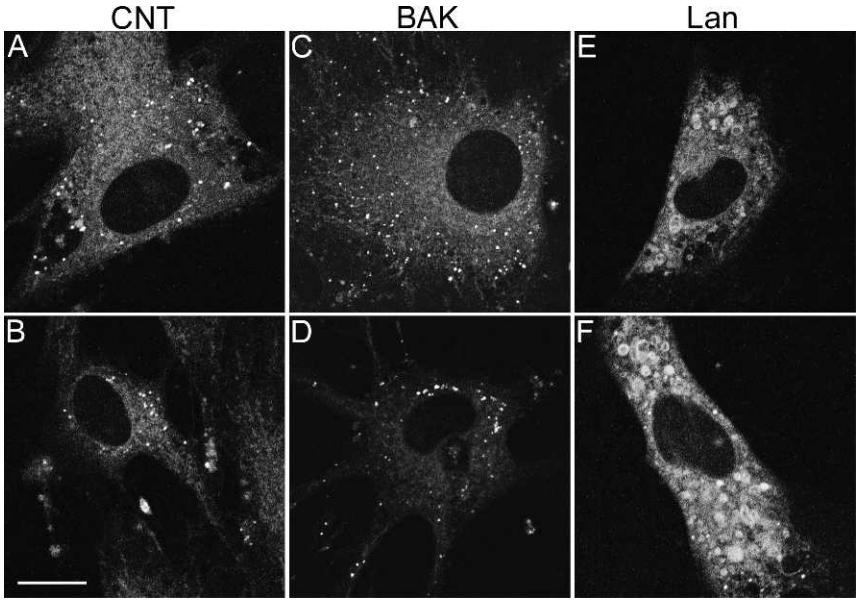

FIGURE 7. Intracellular structures induced by latanoprost treatment also stain with a fluorescent lipophilic dye. Human trabecular meshwork cells were grown for 24 hours in 0.5 μg/mL latanoprost and 2 μg/mL BAK (Lan [**E**, **F**]), in 2 μg/mL BAK (BAK [**C**, **D**]), or with no addition (CNT [**A**, **B**]). Cells were fixed and the lipid structures stained using Nile Red. Round intracellular structures are visible only with Lan treatment (**E**, **F**). *Scale bar*: 20 μm.

corneal angle, and retina within the intact eye.[19,32–37] We have also used the TPAF signal from NAD(P)H to image the time course of oxidative stress in living cultures of hTMC.[10] In this study, we examined hTMC using CARS microscopy in order to detect morphology changes to the lipid membrane of cells and TPAF to detect changes in oxidative state. We hypothesized that latanoprost would induce morphological changes to hTMC that could be consistent with changes to fluid outflow, or possibly other changes that could reflect other cellular functional effects. While we did note rounding of hTMC with simultaneous CARS/TPAF microscopy, we are the first to show that nonconfluent cultures of hTMC form intracellular lipid vesicles after exposure to 0.2 μg/mL latanoprost. We have also used histological staining to determine that latanoprost causes morphological changes to both lipid structures and actin cytoskeleton. These morphological changes were not accompanied by an appreciable change in the density of FA between hTMC and growth substrate. PGA-induced rearrangement of actin filaments and rounding in TM and Schlemm's canal cells could potentially result in changes in AH flow through the conventional pathway. Such a mechanism has been demonstrated by the regulation of the Rho-kinase pathway, which affects the TM cell actin cytoskeleton resulting in changes to TM cell shape that ultimately influence AH outflow.[31] However, the formation of intracellular vesicles is not a direct result of these actin changes, since other agents known to cause hTMC morphological and cytoskeletal changes do not trigger formation of vesicles.

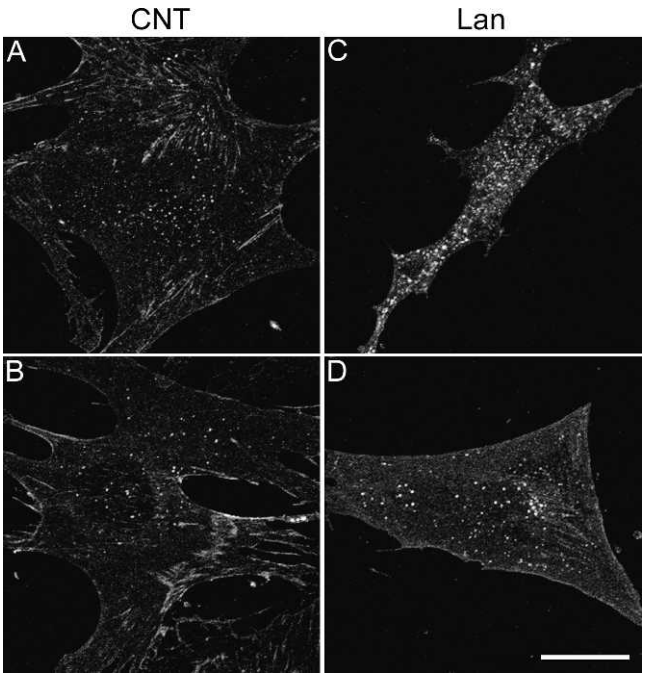

FIGURE 8. Staining of focal adhesions in human trabecular meshwork cells (hTMC). Cells were grown for 24 hours in 0.5 μg/mL latanoprost and 2 μg/mL BAK (Lan [**C**, **D**]) or with no addition (CNT [**A**, **B**]). Cells were fixed and then stained with an antibody for β1 integrin to detect focal adhesions. *Scale bar*: 20 μm.

The function and purpose of these PGA-induced intracellular vesicles is not obvious. Our working hypothesis is that these lipid-based morphological changes are linked to the ability of PGAs to induce release matrix metalloproteinases (MMPs), enzymes that ultimately cause remodeling of collagen within the tissue of the uveoscleral pathway. Synthesis and release of MMPs would involve creation and movement of small (<1 μm) intracellular secretory vesicles, not the large lipid structures noted here. We have no reason to believe that these lipid structures are indicative of cell stress or cell death. Previous studies using ophthalmic formulations of PGAs have demonstrated no cytotoxic effect in cultured TM cells (outside of the toxic effect from the contained BAK preservative).[38,39] Furthermore, preservative-free formulations of PGAs appear to protect cultured TM cells from damage by oxidative stress.[40] However, use of PGAs in perfused eyes causes detachment of some endothelial cells from the inner wall of Schlemm's canal.[41] This is consistent with a loss of focal adhesion

contacts between cell and extracellular matrix, resulting in loss of cell adhesion. Therefore, while PGAs do not appear to be directly cytotoxic, the cytoskeletal and morphological changes that they induce in TM and Schlemm's canal endothelial cells can lead to cell detachment and subsequent death.

To our knowledge, the PGA-induced changes to actin structures and lipid membranes in cultured human TM cells shown here have not been seen before, although other laboratories have microscopically examined PGA effects on TM cells. Zhao et al. examined confluent cultures of human TM cells exposed to latanoprost (10 μg/mL) for 9 days and found no changes under ×20 phase-contrast microscopy, but they did not examine cells at high magnification or attempt to visualize intracellular structures.[42] Alvarado et al. noted an increase in the disassembly of junctions between Schlemm's canal endothelial cells with a 12-hour treatment of 2 μg/mL PGA.[43] No intracellular vesicles were apparent; however, cells of Schlemm's canal function as a continuous endothelial sheet in vivo whereas endothelial cells of the TM do not. Some of the morphological and actin changes noted here are similar to those seen in smooth muscle cells treated for 1 hour with 10 ng/mL PGA.[44] The smooth muscle cells exhibited a rounded appearance and a reduction in both filamentous actin and focal adhesions, but intracellular lipid vesicles were not noted.

The work presented here supports the hypothesis that CARS/TPAF can add a wealth of information on cellular dynamics and interactions without the need for exogenous fluorescent dyes. Further experiments are needed to determine the function of these intracellular lipid structures. For example, fluorescent labeling of the plasma membrane could help determine whether these structures arise from outer or inner cell membranes. Additionally, cell fractionation techniques can be employed to determine the contents of these vesicles. Ultimately we propose that evolving MPM technologies might help determine how these PGA-induced processes are involved in the hypotensive action of PGAs in vivo.

Acknowledgments

Supported by NIH/NCRR Grant S10 RR025447 (institutional core facility grant; coherent anti-Stokes Raman scattering microscope) and NIH/NCRR/Colorado CTSI Grant UL1 RR025780 (Advanced Light Microscopy Core Facility, University of Colorado Denver); NIH/NIDDK Grant K25 DK095232 (TLC).

Disclosure: **T.C. Lei**, P; **O. Masihzadeh**, P; **M.Y. Kahook**, P; **D.A. Ammar**, P

References

1. Orme M, Collins S, Dakin H, Kelly S, Loftus J. Mixed treatment comparison and meta-regression of the efficacy and safety of prostaglandin analogues and comparators for primary open-angle glaucoma and ocular hypertension. *Curr Med Res Opin*. 2010;26:511–528.
2. Aung T, Chan YH, Chew PT; EXACT Study Group. Degree of angle closure and the intraocular pressure-lowering effect of latanoprost in subjects with chronic angle-closure glaucoma. *Ophthalmology*. 2005;112:267–271.
3. Crawford K, Kaufman PL. Pilocarpine antagonizes prostaglandin F2 alpha-induced ocular hypotension in monkeys. Evidence for enhancement of uveoscleral outflow by prostaglandin F2 alpha. *Arch Ophthalmol*. 1987;105:1112–1116.
4. Lutjen-Drecoll E, Tamm E. Morphological study of the anterior segment of cynomolgus monkey eyes following treatment with prostaglandin F2 alpha. *Exp Eye Res*. 1988;47:761–769.
5. Toris CB, Gabelt BT, Kaufman PL. Update on the mechanism of action of topical prostaglandins for intraocular pressure reduction. *Surv Ophthalmol*. 2008;53(suppl 1):S107–S120.
6. Millard LH, Woodward DF, Stamer WD. The role of the prostaglandin EP4 receptor in the regulation of human outflow facility. *Invest Ophthalmol Vis Sci*. 2011;52:3506–3513.
7. Helmchen F, Denk W. Deep tissue two-photon microscopy. *Nat Methods*. 2005;2:932–940.
8. Denk W, Strickler JH, Webb WW. Two-photon laser scanning fluorescence microscopy. *Science*. 1990;248:73–76.
9. Cox G, Sheppard CJ. Practical limits of resolution in confocal and non-linear microscopy. *Microsc Res Tech*. 2004;63:18–22.
10. Masihzadeh O, Ammar DA, Lei TC, Gibson EA, Kahook MY. Real-time measurements of nicotinamide adenine dinucleotide in live human trabecular meshwork cells: effects of acute oxidative stress. *Exp Eye Res*. 2011;93:316–320.
11. Cheng JX, Xie XS. Coherent anti-Stokes Raman scattering microscopy: instrumentation, theory, and applications. *J Phys Chem B*. 2004;108:827–840.
12. Zumbusch A, Holtom GR, Xie XS. Three-dimensional vibrational imaging by coherent anti-Stokes Raman scattering. *Phys Rev Lett*. 1999;82:4142–4145.
13. Potma E, de Boeij WP, van Haastert PJ, Wiersma DA. Real-time visualization of intracellular hydrodynamics in single living cells. *Proc Natl Acad Sci U S A*. 2001;98:1577–1582.
14. Xie XS, Yu J, Yang WY. Living cells as test tubes. *Science*. 2006;312:228–230.
15. Le TT, Huff TB, Cheng JX. Coherent anti-Stokes Raman scattering imaging of lipids in cancer metastasis. *BMC Cancer*. 2009;9:42.
16. Nan X, Cheng JX, Xie XS. Vibrational imaging of lipid droplets in live fibroblast cells with coherent anti-Stokes Raman scattering microscopy. *J Lipid Res*. 2003;44:2202–2208.
17. Nan X, Potma EO, Xie XS. Nonperturbative chemical imaging of organelle transport in living cells with coherent anti-stokes Raman scattering microscopy. *Biophys J*. 2006;91:728–735.
18. Tong L, Lu Y, Lee RJ, Cheng JX. Imaging receptor-mediated endocytosis with a polymeric nanoparticle-based coherent anti-stokes Raman scattering probe. *J Phys Chem B*. 2007;111:9980–9985.
19. Lei TC, Ammar DA, Masihzadeh O, Gibson EA, Kahook MY. Label-free imaging of trabecular meshwork cells using Coherent Anti-Stokes Raman Scattering (CARS) microscopy. *Mol Vis*. 2011;17:2628–2633.
20. Potma E. Tissue imaging with coherent anti-Stokes Raman scattering microscopy. In: Srinivasan G, ed. *Vibrational Spectroscopy Imaging for Biomedical Application*. New York: McGraw-Hill Professional; 2010;319–348.
21. Hudson BD, Kelly ME. Identification of novel competing beta2AR phospho-extracellular signal regulated kinase 1/2 signaling pathways in human trabecular meshwork cells. *J Ocul Pharmacol Ther*. 2012;28:17–25.
22. Polansky JR, Fauss DJ, Chen P, et al. Cellular pharmacology and molecular biology of the trabecular meshwork inducible glucocorticoid response gene product. *Ophthalmologica*. 1997;211:126–139.
23. Dismuke WM, Mbadugha CC, Faison D, Ellis DZ. Ouabain-induced changes in aqueous humour outflow facility and trabecular meshwork cytoskeleton. *Br J Ophthalmol*. 2009;93:104–109.
24. Vincent S, Settleman J. Inhibition of RhoGAP activity is sufficient for the induction of Rho-mediated actin reorganization. *Eur J Cell Biol*. 1999;78:539–548.
25. Tian B, Gabelt BT, Geiger B, Kaufman PL. The role of the actomyosin system in regulating trabecular fluid outflow. *Exp Eye Res*. 2009;88:713–717.

Investigative Ophthalmology & Visual Science

26. Klinkner AM, Bugelski PJ, Waites CR, Louden C, Hart TK, Kerns WD. A novel technique for mapping the lipid composition of atherosclerotic fatty streaks by en face fluorescence microscopy. *J Histochem Cytochem*. 1997;45: 743–753.
27. Aga M, Bradley JM, Keller KE, Kelley MJ, Acott TS. Specialized podosome- or invadopodia-like structures (PILS) for focal trabecular meshwork extracellular matrix turnover. *Invest Ophthalmol Vis Sci*. 2008;49:5353–5365.
28. Filla MS, Woods A, Kaufman PL, Peters DM. Beta1 and beta3 integrins cooperate to induce syndecan-4-containing cross-linked actin networks in human trabecular meshwork cells. *Invest Ophthalmol Vis Sci*. 2006;47:1956–1967.
29. Diskin S, Chen WS, Cao Z, et al. Galectin-8 promotes cytoskeletal rearrangement in trabecular meshwork cells through activation of Rho signaling. *PLoS One*. 2012;7: e44400.
30. Potma EO, de Boeij WP, Wiersma DA. Nonlinear coherent four-wave mixing in optical microscopy. *J Opt Soc Am B*. 2000;17: 1678–1684.
31. Rao PV, Deng P, Sasaki Y, Epstein DL. Regulation of myosin light chain phosphorylation in the trabecular meshwork: role in aqueous humour outflow facility. *Exp Eye Res*. 2005;80: 197–206.
32. Ammar DA, Lei TC, Gibson EA, Kahook MY. Two-photon imaging of the trabecular meshwork. *Mol Vis*. 2010;16:935–944.
33. Johnson AW, Ammar DA, Kahook MY. Two-photon imaging of the mouse eye. *Invest Ophthalmol Vis Sci*. 2011;52:4098–4105.
34. Masihzadeh O, Ammar DA, Kahook MY, Gibson EA, Lei TC. Direct trabecular meshwork imaging in porcine eyes through multiphoton gonioscopy. *J Biomed Opt*. 2013;18:036009.
35. Masihzadeh O, Ammar DA, Kahook MY, Lei TC. Coherent anti-Stokes Raman scattering (CARS) microscopy: a novel technique for imaging the retina. *Invest Ophthalmol Vis Sci*. 2013; 54:3094–3101.
36. Ammar DA, Lei TC, Kahook MY, Masihzadeh O. Imaging the intact mouse cornea by coherent anti-Stokes Raman scattering (CARS). *Invest Ophthalmol Vis Sci*. 2013;54:5258–5265.
37. Masihzadeh O, Lei TC, Ammar DA, Kahook MY, Gibson EA. A multiphoton microscope platform for imaging the mouse eye. *Mol Vis*. 2012;18:1840–1848.
38. Ammar DA, Kahook MY. Effects of glaucoma medications and preservatives on cultured human trabecular meshwork and non-pigmented ciliary epithelial cell lines. *Br J Ophthalmol*. 2011;95:1466–1469.
39. Hamard P, Blondin C, Debbasch C, Warnet JM, Baudouin C, Brignole F. In vitro effects of preserved and unpreserved antiglaucoma drugs on apoptotic marker expression by human trabecular cells. *Graefes Arch Clin Exp Ophthalmol*. 2003; 241:1037–1043.
40. Yu AL, Fuchshofer R, Kampik A, Welge-Lussen U. Effects of oxidative stress in trabecular meshwork cells are reduced by prostaglandin analogues. *Invest Ophthalmol Vis Sci*. 2008;49: 4872–4880.
41. Bahler CK, Howell KG, Hann CR, Fautsch MP, Johnson DH. Prostaglandins increase trabecular meshwork outflow facility in cultured human anterior segments. *Am J Ophthalmol*. 2008;145:114–119.
42. Zhao X, Pearson KE, Stephan DA, Russell P. Effects of prostaglandin analogues on human ciliary muscle and trabecular meshwork cells. *Invest Ophthalmol Vis Sci*. 2003; 44:1945–1952.
43. Alvarado JA, Iguchi R, Martinez J, Trivedi S, Shifera AS. Similar effects of selective laser trabeculoplasty and prostaglandin analogs on the permeability of cultured Schlemm canal cells. *Am J Ophthalmol*. 2010;150:254–264.
44. Bulin C, Albrecht U, Bode JG, et al. Differential effects of vasodilatory prostaglandins on focal adhesions, cytoskeletal architecture, and migration in human aortic smooth muscle cells. *Arterioscler Thromb Vasc Biol*. 2005;25:84–89.

Investigative Ophthalmology & Visual Science